

# DeLS-SPEC: DECOUPLED LONG-SHORT CONTEXTS FOR PARALLEL SPECULATIVE DRAFTING

Hong-Kai Zheng, Piji Li \*

College of Artificial Intelligence,

Nanjing University of Aeronautics and Astronautics, China

MIIT Key Laboratory of Pattern Analysis and Machine Intelligence, Nanjing, China

The Key Laboratory of Brain-Machine Intelligence Technology,

Ministry of Education, Nanjing, China

{dt.ttt, pjli}@nuaa.edu.cn

## ABSTRACT

Speculative decoding accelerates LLM inference by drafting multiple tokens and verifying them in parallel. Block-parallel drafters such as DFlash further improve drafting efficiency by predicting an entire block in one pass, but their position-wise predictions lack explicit intra-block causal conditioning. Recent methods such as Domino and DSpark attempt to introduce such causality into block-parallel drafting, but they require training the draft model from scratch, which limits their flexibility and increases training cost. We propose **DeLS-Spec**, a decoupled long-short context speculative decoding method. DeLS-Spec treats the fixed DFlash model as a long-context expert and introduces a lightweight local head as a short-context expert. The local head can be trained independently with a standard next-token prediction objective, without joint training with the target model or the DFlash backbone, leading to extremely low training cost. At inference time, DeLS-Spec combines long-context and short-context logits, and the local head is not tied to a specific DFlash checkpoint, making the method more modular and flexible. Experiments on Qwen3 models show that DeLS-Spec consistently improves speedup and average acceptance length over DFlash across math, code, and dialogue benchmarks. Code is available at GitHub.

## 1 INTRODUCTION

Large language models are typically decoded autoregressively (Achiam et al., 2023; Liu et al., 2024; Yang et al., 2025), where each generated token requires a new forward pass of the target model. This sequential process becomes a major latency bottleneck, especially for long-form generation and interactive applications. Speculative decoding mitigates this problem by using a lightweight draft model to propose multiple future tokens, which are then verified in parallel by the target model while preserving the target distribution (Leviathan et al., 2023; Chen et al., 2023).

The efficiency of speculative decoding depends heavily on the drafter (Cai et al., 2024; Ankner et al., 2024; Li et al., 2024a;b; 2026b). Traditional autoregressive drafters maintain strong local consistency but still generate draft tokens sequentially (Li et al., 2024a; Cheng et al., 2024). Recent block-parallel drafters, such as DFlash, improve drafting efficiency by predicting an entire block of tokens in one pass (An et al., 2025; Liu et al., 2026; Chen et al., 2026). However, this parallelism also introduces a limitation: tokens inside the same draft block are predicted largely independently, without explicitly conditioning on previously drafted tokens in that block (Chen et al., 2026; Huang et al., 2026; Rheinboldt et al., 2026). As a result, DFlash provides strong long-context predictions from the prefix, but lacks explicit short-context causal modeling within the draft block.

Several recent methods, including Domino and DSpark, attempt to address this issue by introducing intra-block causality into block-parallel drafting (Huang et al., 2026; Cheng et al., 2026b; Hu et al., 2026; Rheinboldt et al., 2026). These methods show that modeling causal dependencies inside the

---

\*Corresponding author

draft block can improve acceptance. However, they usually require training a new draft model from scratch or jointly training the draft backbone with additional causal components. This makes them costly to apply when a DFlash-style drafter has already been trained, and limits their flexibility across different draft checkpoints.

In this work, we propose **DeLS-Spec**, a decoupled long-short context speculative decoding method. Instead of modifying or retraining the DFlash backbone (Chen et al., 2026), DeLS-Spec keeps DFlash fixed as a long-context expert and introduces a lightweight local head as a short-context expert. The DFlash expert captures semantic and task-level information from the full prefix, while the local head captures causal dependencies from the already drafted tokens inside the current block.

A key property of DeLS-Spec is its decoupled training. The local head is trained independently with a standard next-token prediction objective on plain text data. It does not require target-model hidden states, DFlash hidden states, or joint optimization with the speculative decoding pipeline. This makes training extremely cheap and allows the local head to be attached to existing DFlash-style checkpoints after they have been trained. At inference time, DeLS-Spec combines the long-context logits from DFlash and the short-context logits from the local head (Hinton, 2002). Since the local head is not trained together with a specific DFlash checkpoint, it is not one-to-one tied to the DFlash weights during inference. This makes the method more modular and flexible: a trained local head can be reused or transferred across compatible DFlash checkpoints, rather than requiring a new draft model to be trained for each setting.

We evaluate DeLS-Spec on Qwen3 models (Yang et al., 2025) across math, code, and dialogue benchmarks. Experiments show that DeLS-Spec consistently improves both decoding speedup and average acceptance length over DFlash. These results demonstrate that decoupling long-context block-parallel drafting from short-context causal correction is an efficient and practical way to enhance existing speculative decoding systems.

Our contributions are summarized as follows:

- We propose DeLS-Spec, a decoupled long-short context speculative decoding method that improves DFlash-style block-parallel drafting without retraining the DFlash backbone.
- We introduce a lightweight local head that provides intra-block causal information and can be trained independently with a standard next-token prediction objective.
- DeLS-Spec consistently enhances DFlash on Qwen3 models across math, code, and dialogue benchmarks, while offering modular flexibility across different checkpoints.

## 2 RELATED WORK

**Speculative decoding and classical drafters.** Speculative decoding accelerates autoregressive inference by using a lightweight drafter to propose multiple tokens and a target model to verify them in parallel while preserving the target distribution (Leviathan et al., 2023; Chen et al., 2023). Early blockwise decoding and tree-based verification reduce sequential decoding rounds or expand candidate coverage (Stern et al., 2018; Miao et al., 2024). Later drafters improve proposal quality through target-attached heads, sequentially dependent heads, feature-level drafting, dynamic draft trees, recurrent drafting, and distillation (Cai et al., 2024; Ankner et al., 2024; Li et al., 2024a;b; 2026b; Cheng et al., 2024; Zhou et al., 2024). However, many drafters still require sequential drafting, feature updates, or tree construction, making drafting cost grow with the speculative budget.

**Parallel and diffusion-based drafting.** Parallel generation reduces drafting latency by predicting multiple positions simultaneously, but also weakens token dependency, as observed in non-autoregressive and diffusion-style language generation (Gu et al., 2017; Nie et al., 2026; Arriola et al., 2025; Cheng et al., 2026a; Liu et al., 2025). Recent speculative drafters therefore use diffusion or parallel prediction to generate draft blocks efficiently (Christopher et al., 2025; Li et al., 2026a; Sandler et al., 2025; An et al., 2025; Liu et al., 2026). DFlash is most relevant to our work: it uses a lightweight block-diffusion drafter with target hidden-state injection to obtain strong long-context conditioning and generate a whole block in one pass (Chen et al., 2026). Follow-up methods build draft trees or improve training objectives for such parallel drafters (Ringel & Romano, 2026; Wu et al., 2026). Nevertheless, DFlash-style block-parallel prediction mainly models position-wise

long-context distributions and lacks explicit conditioning on the locally drafted prefix, which can hurt later-token acceptance.

**Intra-block causality and parallel-drafter correction.** Several methods address the missing local causality in parallel drafting. Hydra introduces dependency among draft heads (Ankner et al., 2024); Domino corrects DFlash-style logits with a GRU causal encoder and low-rank residual head (Huang et al., 2026); DSpark adds semi-autoregressive Markov/RNN heads and confidence scheduling (Cheng et al., 2026b); JetSpec uses tree-causal attention for branch-wise causal conditioning (Hu et al., 2026); and TreeFlash approximates local autoregressive distributions on top of DFlash (Rheinboldt et al., 2026). D-PACE further shows that accepted length is tied to position-dependent prefix acceptance (Wu et al., 2026). Although structured non-autoregressive decoding and CTC-based drafting can introduce dependencies or alignments (Sun et al., 2019; Wen et al., 2024), they are less compatible with the exact per-position probabilities required by standard lossless verification. Unlike these unified correction pipelines, DeLS-Spec keeps the trained DFlash drafter fixed as a long-context expert, independently trains a lightweight short-context expert for intra-block causality, and fuses their logits with unigram-prior correction to avoid double-counting frequency bias.

### 3 PRELIMINARIES

#### 3.1 PARALLEL DRAFT MODEL: DFLASH

Let  $y = x_{<k}$  denote the observed long context, and let  $x_k, x_{k+1}, \dots, x_{k+s}$  denote the block of future tokens to be drafted. Parallel draft models such as DFlash (Chen et al., 2026) perform block-parallel drafting by predicting multiple future tokens in a single forward pass. Specifically, for each position inside the draft block, the model predicts

$$p_L(x_i | y), \quad i \in \{k, \dots, k+s\}. \quad (1)$$

Although DFlash is described as a diffusion language model, its practical drafting procedure consists of one forward pass followed by one sampling step, which can be viewed as a diffusion language model with a single denoising step. This design significantly reduces draft latency compared with autoregressive draft models. However, because tokens within the block are predicted in parallel, each position is unaware of the tokens generated at other positions. As a result, the causal dependency inside the draft block is weak, which limits the accepted length during speculative decoding.

#### 3.2 INTRODUCING INTRA-BLOCK CAUSALITY

Recent approaches such as Domino (Huang et al., 2026) and DSpark (Cheng et al., 2026b) address this issue by introducing intra-block causal modeling on top of the parallel DFlash backbone. They attach a lightweight causal correction head after the parallel backbone and directly optimize

$$\mathcal{L}_{cc} = - \sum_{i=k+1}^{k+s} \log p(x_i | y, z_i), \quad z_i = x_{k:i-1}. \quad (2)$$

where  $z_i$  denotes the local prefix within the draft block. Although this causal correction improves local consistency, it is typically trained as part of the complete draft pipeline. In particular, it depends on the target model and requires joint training or fine-tuning of the parallel DFlash backbone and the causal correction head. Therefore, migrating such causal dependency mechanisms to an already trained DFlash model can be expensive, especially when the model size increases.

## 4 METHOD

### 4.1 DECOUPLED LONG-SHORT CONTEXTS

We propose **DeLS-Spec**, a decoupled long-short context modeling method for speculative drafting. The key observation is that an already trained DFlash model provides a long-context conditional distribution  $p_L(x_i | y)$ , which captures semantic and task-level constraints from the full prefix  $y$ .



**Algorithm 1** DeLS-Spec Inference

---

**Require:** Target model  $M_T$ , DFlash draft model  $M_L$ , local head  $M_S$ , unigram-prior logits  $\ell_P$ , fusion weights  $\alpha, \beta$ , draft span  $s$ , initial prefix  $y$

**Ensure:** Generated continuation appended to  $y$

- 1: **while** not finished **do**
- 2:   Get DFlash logits:  $\{\ell_L^{(j)}\}_{j=0}^s \leftarrow M_L(y)$ .
- 3:   Sample the first draft token:  $x_0 \sim \text{Decode}(\text{softmax}(\ell_L^{(0)}))$ .
- 4:   **for**  $j = 1$  to  $s$  **do**
- 5:     Get short-context logits:  $\ell_S^{(j)} \leftarrow M_S(x_{0:j-1})$ .
- 6:     Fuse logits:  $\ell^{(j)} = \ell_L^{(j)} + \alpha \ell_S^{(j)} - \beta \ell_P$ .
- 7:     Sample draft token:  $x_j \sim \text{Decode}(\text{softmax}(\ell^{(j)}))$ .
- 8:   **end for**
- 9:   Verify  $(x_0, \dots, x_s)$  with one target-model forward pass.
- 10:   Append accepted tokens and the bonus token, if any, to  $y$ .
- 11: **end while**
- 12: **return**  $y$

---

In contrast, DeLS-Spec deliberately ignores this residual term in exchange for modularity and training efficiency. We approximate

$$\log p(x_i | y, z_i) \approx \log p_L(x_i | y) + \log p_S(x_i | z_i) - \log p_P(x_i), \quad (8)$$

where  $p_L$  is the long-context distribution provided by the trained DFlash model,  $p_S$  is an independently trained short-context model, and  $p_P$  is the unigram prior estimated from the training corpus.

#### 4.2 INDEPENDENT SHORT-CONTEXT TRAINING

A key advantage of DeLS-Spec is that the short-context model can be trained completely independently. It does not require hidden states from the target model, nor does it require access to the DFlash draft model. The only requirement is that it shares the same tokenizer as the target model. In our implementation,  $p_S(x_i | z_i)$  is parameterized by a lightweight local RNN head and trained on plain text corpora with the standard next-token prediction objective:

$$\mathcal{L}_S = - \sum_{i=k+1}^{k+s} \log p_S(x_i | z_i), \quad z_i = x_{k:i-1}. \quad (9)$$

This training objective encourages the short-context model to capture local causal dependencies inside a draft block, independent of the long-context drafting model.

#### 4.3 LOGIT FUSION AT INFERENCE

During inference, DeLS-Spec is directly attached to an already trained DFlash draft model. Let  $\ell_L(x_i | y)$  denote the long logits produced by DFlash,  $\ell_S(x_i | z_i)$  denote the short logits produced by the local RNN head, and  $\ell_P(x_i)$  denote the log unigram prior estimated from the training corpus. We fuse these logits as

$$\ell(x_i) = \ell_L(x_i | y) + \alpha \ell_S(x_i | z_i) - \beta \ell_P(x_i), \quad (10)$$

where  $\alpha$  and  $\beta$  are calibration coefficients. The theoretical decomposition corresponds to  $\alpha = \beta = 1$ . In practice, however, the long logits, short logits, and unigram prior are obtained from different sources and may have different scales. Therefore,  $\alpha$  and  $\beta$  are introduced to calibrate their relative contributions. The unigram prior term  $\ell_P(x_i)$  is computed once from corpus statistics and introduces no additional inference-time model computation, its estimation details are provided in Appendix A. The complete inference procedure is summarized in Figure 1 and Algorithm 1.

## 5 EXPERIMENTS

### 5.1 EXPERIMENTAL SETUP

**Models and Benchmarks.** We evaluate DeLS-Spec on Qwen3-4B and Qwen3-8B (Yang et al., 2025). For the DFlash backbone (Chen et al., 2026), we use the officially released checkpoints `z-lab/Qwen3-4B-DFlash-b16` and `z-lab/Qwen3-8B-DFlash-b16`, both with a draft block size of 16. We evaluate on math reasoning, code generation, and open-ended dialogue benchmarks. The math benchmarks include GSM8K (Cobbe et al., 2021), MATH-500 (Hendrycks et al., 2021), and AIME25 (Zhang & Math-AI, 2025); the code benchmarks include HumanEval (Chen et al., 2021), MBPP (Austin et al., 2021), and LiveCodeBench (Jain et al., 2025); and the dialogue benchmarks include MT-Bench (Zheng et al., 2023) and Alpaca (Taori et al., 2023). We report end-to-end decoding speedup over autoregressive decoding and the average acceptance length  $\tau$ .

**Training Data.** We use the DFlash authors’ `Qwen3-4B-Instruct-100K` data (Chen et al., 2026) for the 4B setting and the Domino authors’ `Qwen3-8B-ShareGPT` data (Huang et al., 2026) for the 8B setting. These corpora are used both to train the local head and to estimate the unigram prior. Unlike methods that jointly fine-tune the draft pipeline, DeLS-Spec only trains the local head with the standard next-token prediction objective on the training corpus. The DFlash backbone used during evaluation is kept fixed and directly loaded from the released `z-lab` checkpoints.

**Baselines.** We compare DeLS-Spec with autoregressive decoding and representative speculative decoding baselines, including EAGLE-3, DART, and DFlash (Li et al., 2026b; Liu et al., 2026; Chen et al., 2026). DFlash is the block-parallel backbone on which DeLS-Spec is built. We also include additional comparisons with Domino-style fine-tuning and other DFlash settings where applicable.

**Implementation.** Unless otherwise specified, all results are evaluated with the Hugging Face Transformers backend (Wolf et al., 2019). All training and evaluation runs are conducted on a single NVIDIA L20 GPU. The local head is implemented as a GRU-based RNN by default. For DeLS-Spec inference, we set  $\alpha = \beta = 0.3$  unless otherwise stated. Following Domino, we optimize the inference implementation with CUDA Graphs and fused Triton kernels (Tillet et al., 2019) to reduce the overhead of the local-head decoding loop. Detailed local-head training hyperparameters are provided in Table 6.

### 5.2 MAIN RESULTS

Table 1 presents the main results on Qwen3-4B and Qwen3-8B across math, code, and chat benchmarks. DFlash already outperforms tree-based baselines such as EAGLE-3 and DART by a large margin. Built upon this strong baseline, DeLS-Spec further improves both decoding speedup and average acceptance length  $\tau$  in almost all settings.

The gains are particularly clear on math and code tasks, where local token dependencies are stronger. For Qwen3-4B at temperature 0, DeLS-Spec improves the speedup of DFlash from  $4.74\times$  to  $5.02\times$  on MBPP, from  $6.09\times$  to  $6.35\times$  on MATH-500, and from  $5.69\times$  to  $5.95\times$  on AIME25. Meanwhile, the acceptance length increases by up to 0.44 on AIME25 and 0.40 on MATH-500. Under stochastic decoding, DeLS-Spec also brings notable improvements, e.g., on Qwen3-4B at temperature 1, HumanEval speedup increases from  $4.61\times$  to  $4.85\times$ , with  $\tau$  improved from 5.84 to 6.21. Similar trends hold for Qwen3-8B, where DeLS-Spec improves  $\tau$  by 0.33 on HumanEval and MBPP at temperature 0, and by 0.29 on MT-Bench at temperature 1.

These results show that DeLS-Spec complements DFlash by improving the local consistency of draft tokens. The local head enables more drafted tokens to be accepted during verification, especially on math and code benchmarks, while preserving the original DFlash parallel drafting process.

### 5.3 GENERAL ADAPTABILITY OF THE DELS-SPEC LOCAL HEAD

We further test the general adaptability of the local head on two DFlash block-7 checkpoints from DSpark (Cheng et al., 2026b): `deepseek-ai/dflash-qwen3.4b_block7` and `deepseek-ai/dflash-qwen3.8b_block7`. This setting examines whether the local head can

Table 1: Decoding speedup over vanilla autoregressive decoding and average acceptance length ( $\tau$ ) on Qwen3 models with a maximum of 2048 generated tokens. Parenthesized values indicate the draft tree size for EAGLE-3 and DART, and the draft block size for DFlash and DeLS-Spec. The average is computed over all listed benchmarks.

Model	Method	MATH						CODE						CHAT				OVERALL	
		GSM8K		MATH-500		AIME25		HumanEval		MBPP		LCB		MT-Bench		Alpaca		Avg.	
Temperature = 0		Speedup	$\tau$	Speedup	$\tau$	Speedup	$\tau$	Speedup	$\tau$	Speedup	$\tau$	Speedup	$\tau$	Speedup	$\tau$	Speedup	$\tau$	Speedup	$\tau$
4B	EAGLE-3 (16)	2.24×	3.32	2.10×	3.11	2.08×	3.10	2.09×	3.09	2.02×	2.99	1.95×	2.93	1.95×	2.94	1.87×	2.83	2.04×	3.04
	EAGLE-3 (60)	2.57×	3.83	2.40×	3.59	2.36×	3.53	2.36×	3.53	2.30×	3.44	2.19×	3.31	2.25×	3.41	2.14×	3.29	2.32×	3.49
	DART (60)	2.16×	2.65	2.20×	2.63	2.13×	2.59	2.48×	2.99	2.47×	3.01	2.23×	2.76	2.19×	2.69	2.16×	2.78	2.25×	2.76
	DFlash (16)	5.15×	6.51	6.09×	7.81	5.69×	7.32	5.19×	6.56	4.74×	6.14	5.25×	6.82	2.72×	4.13	2.23×	3.06	4.63×	6.04
	DeLS-Spec (16)	<b>5.29×</b>	<b>6.80</b>	<b>6.35×</b>	<b>8.21</b>	<b>5.95×</b>	<b>7.76</b>	<b>5.42×</b>	<b>6.92</b>	<b>5.02×</b>	<b>6.47</b>	<b>5.50×</b>	<b>7.20</b>	<b>2.77×</b>	<b>4.30</b>	<b>2.25×</b>	<b>3.15</b>	<b>4.82×</b>	<b>6.35</b>
8B	EAGLE-3 (16)	2.21×	3.27	2.09×	3.10	2.07×	3.07	2.17×	3.21	1.93×	2.86	1.80×	2.95	1.82×	2.75	1.67×	2.53	1.97×	2.97
	EAGLE-3 (60)	2.56×	3.80	2.42×	3.61	2.41×	3.59	2.50×	3.74	2.22×	3.31	2.03×	3.12	2.07×	3.17	1.88×	2.90	2.26×	3.41
	DART (60)	2.28×	2.71	2.29×	2.70	2.11×	2.59	2.52×	2.95	2.39×	2.98	2.24×	2.78	2.27×	3.03	2.21×	2.84	2.29×	2.82
	DFlash (16)	4.96×	6.59	5.83×	7.85	5.20×	7.05	4.98×	6.60	4.56×	6.08	5.15×	7.17	2.59×	4.16	2.16×	3.11	4.43×	6.08
	DeLS-Spec (16)	<b>5.08×</b>	<b>6.84</b>	<b>5.98×</b>	<b>8.15</b>	<b>5.40×</b>	<b>7.35</b>	<b>5.16×</b>	<b>6.93</b>	<b>4.72×</b>	<b>6.41</b>	<b>5.16×</b>	<b>7.27</b>	<b>2.66×</b>	<b>4.35</b>	<b>2.18×</b>	<b>3.20</b>	<b>4.54×</b>	<b>6.31</b>
Temperature = 1		Speedup	$\tau$	Speedup	$\tau$	Speedup	$\tau$	Speedup	$\tau$	Speedup	$\tau$	Speedup	$\tau$	Speedup	$\tau$	Speedup	$\tau$	Speedup	$\tau$
4B	EAGLE-3 (16)	2.18×	3.26	2.00×	3.00	1.86×	2.80	2.02×	3.04	1.97×	2.95	1.87×	2.83	1.90×	2.91	1.78×	2.72	1.95×	2.94
	EAGLE-3 (60)	2.44×	3.77	2.28×	3.51	2.08×	3.10	2.09×	3.09	2.19×	3.38	2.05×	3.19	2.11×	3.33	2.02×	3.17	2.16×	3.32
	DART (60)	2.19×	2.65	2.20×	2.63	2.13×	2.59	2.48×	2.99	2.46×	3.01	2.23×	2.76	2.19×	2.69	2.16×	2.78	2.26×	2.76
	DFlash (16)	4.69×	5.95	5.02×	6.59	3.69×	4.90	4.61×	5.84	4.43×	5.68	5.06×	6.66	<b>2.61×</b>	3.89	2.12×	2.90	4.03×	5.30
	DeLS-Spec (16)	<b>4.82×</b>	<b>6.22</b>	<b>5.14×</b>	<b>6.99</b>	<b>3.81×</b>	<b>5.04</b>	<b>4.85×</b>	<b>6.21</b>	<b>4.58×</b>	<b>5.89</b>	<b>5.15×</b>	<b>6.79</b>	2.59×	<b>3.94</b>	<b>2.16×</b>	<b>3.00</b>	<b>4.14×</b>	<b>5.51</b>
8B	EAGLE-3 (16)	2.18×	3.26	1.96×	3.00	1.86×	2.80	2.05×	3.09	1.97×	2.95	1.90×	2.93	1.91×	2.91	1.78×	2.83	1.95×	2.97
	EAGLE-3 (60)	2.40×	3.70	2.23×	3.44	2.05×	3.17	2.32×	3.58	2.11×	3.24	1.90×	2.95	1.91×	3.02	1.78×	2.81	2.09×	3.24
	DART (60)	2.25×	2.71	2.25×	2.70	2.13×	2.59	2.45×	2.95	2.45×	2.98	2.25×	2.78	2.24×	2.73	2.18×	2.84	2.28×	2.79
	DFlash (16)	4.40×	5.88	4.69×	6.48	3.27×	4.57	4.13×	5.48	4.01×	5.36	4.84×	6.79	2.38×	3.73	2.03×	2.93	3.72×	5.15
	DeLS-Spec (16)	<b>4.51×</b>	<b>6.09</b>	<b>4.78×</b>	<b>6.73</b>	<b>3.36×</b>	<b>4.82</b>	<b>4.26×</b>	<b>5.75</b>	<b>4.12×</b>	<b>5.64</b>	<b>4.96×</b>	<b>6.96</b>	<b>2.44×</b>	<b>4.02</b>	<b>2.04×</b>	<b>2.96</b>	<b>3.81×</b>	<b>5.37</b>

Table 2: Results of directly applying DeLS-Spec to DSpark’s DFlash block-7 checkpoints. DeLS-Spec achieves consistent performance improvements across all benchmarks.

Model	Method	GSM8K		MATH-500		AIME25		HumanEval		MBPP		LCB		MT-Bench		Alpaca		Avg.	
		Speedup	$\tau$	Speedup	$\tau$	Speedup	$\tau$	Speedup	$\tau$	Speedup	$\tau$	Speedup	$\tau$	Speedup	$\tau$	Speedup	$\tau$	Speedup	$\tau$
4B	DFlash	4.03×	4.93	3.79×	4.65	3.21×	3.93	3.10×	3.75	3.38×	4.13	3.25×	3.96	2.43×	3.17	2.26×	2.87	3.18×	3.92
	DeLS-Spec	<b>4.24×</b>	<b>5.20</b>	<b>4.05×</b>	<b>4.96</b>	<b>3.47×</b>	<b>4.21</b>	<b>3.36×</b>	<b>4.08</b>	<b>3.59×</b>	<b>4.42</b>	<b>3.44×</b>	<b>4.23</b>	<b>2.53×</b>	<b>3.37</b>	<b>2.34×</b>	<b>3.00</b>	<b>3.38×</b>	<b>4.18</b>
8B	DFlash	4.05×	4.84	3.73×	4.49	3.29×	3.87	3.10×	3.68	3.44×	4.13	3.38×	4.04	2.49×	3.23	2.34×	2.91	3.23×	3.90
	DeLS-Spec	<b>4.21×</b>	<b>5.16</b>	<b>3.91×</b>	<b>4.81</b>	<b>3.36×</b>	<b>4.08</b>	<b>3.26×</b>	<b>3.97</b>	<b>3.55×</b>	<b>4.34</b>	<b>3.53×</b>	<b>4.35</b>	<b>2.56×</b>	<b>3.39</b>	<b>2.40×</b>	<b>3.05</b>	<b>3.35×</b>	<b>4.14</b>

transfer beyond our default DFlash configuration. Since the local head is trained with block size 16, it can be directly used with DFlash models whose block size is no larger than 16.

As shown in Table 2, DeLS-Spec consistently improves these DSpark checkpoints. On the 4B checkpoint, DeLS-Spec brings speedup gains on MATH-500, AIME25, and HumanEval, improving DFlash by 0.26× on each benchmark. It also increases the acceptance length by 0.33 on HumanEval and 0.31 on MATH-500. On the 8B checkpoint, DeLS-Spec improves  $\tau$  by 0.32 on GSM8K and MATH-500, and by 0.31 on LCB, while also increasing speedup across all benchmarks.

These consistent improvements on independently released block-7 checkpoints demonstrate that the DeLS-Spec local head is not tied to a specific DFlash implementation. Instead, it can serve as a plug-in module that improves local draft-token modeling for different DFlash-style draft models.

#### 5.4 EFFECT OF $\alpha$ AND $\beta$

We further study the effect of the two combination hyperparameters,  $\alpha$  and  $\beta$ , by performing a grid search on Qwen3-4B. Figure 2 summarizes the results. The left panel shows that  $\alpha$  and  $\beta$  should be increased jointly to achieve the best performance, rather than tuning either one alone. The heatmap also exhibits a clear diagonal trend, suggesting that in practice  $\alpha$  and  $\beta$  can simply be set to the same value, with values below 0.5 yielding the best performance. In particular, the best region lies around  $\alpha \approx 0.3$  and  $\beta \approx 0.3$ , indicating that a balanced contribution from the local head and the unigram-prior correction is important.

To better highlight the importance of subtracting the unigram prior, the middle panel normalizes each row by subtracting the corresponding value at  $\beta = 0$ . This row-wise comparison makes the effect of  $\beta$  more explicit: once  $\alpha$  is properly set, using a positive  $\beta$  consistently improves the acceptance

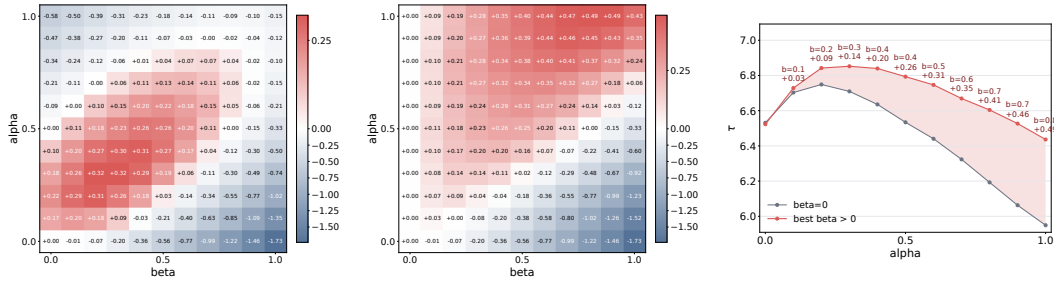


Figure 2:  $\alpha$ ,  $\beta$  scan on Qwen3-4B. Left: average acceptance length under different  $\alpha$  and  $\beta$  values. Middle: row-wise improvement after subtracting the corresponding  $\beta = 0$  value. Right: improvement of the best  $\beta$  for each  $\alpha$  over  $\beta = 0$ .

Table 3: Average acceptance length comparison for estimating the impact of the omitted residual term. The gain ratio reports how much of the Domino-FT improvement over DFlash is recovered by DeLS-Spec without explicitly learning the residual term.

Method	GSM8K	MATH-500	AIME25	HumanEval	MBPP	LCB	MT-Bench	Alpaca	Avg.
DFlash	6.51	7.81	7.32	6.56	6.14	6.82	4.13	3.06	6.04
DeLS-Spec (Markov)	6.69	8.17	7.69	6.82	6.38	7.09	4.29	3.12	6.28
DeLS-Spec (RNN)	6.80	8.21	7.76	6.92	6.47	7.20	4.30	3.15	6.35
Domino-FT	7.03	8.37	7.85	7.01	6.60	7.18	4.37	3.19	6.45
$\tau$ gain ratio	55.77%	71.43%	83.02%	80.00%	71.74%	105.56%	70.83%	69.23%	75.69%

length over the  $\beta = 0$  case. The right panel further summarizes this trend by plotting, for each  $\alpha$ , the improvement of the best  $\beta$  over  $\beta = 0$ . We observe consistent gains across almost all  $\alpha$  values, which confirms that unigram-prior subtraction is a key component of the proposed formulation.

### 5.5 IMPACT OF THE OMITTED RESIDUAL TERM

We next quantify how much performance is lost by omitting the residual term  $R(x_i; y, z_i)$  in DeLS-Spec. Table 3 compares several variants in terms of average acceptance length  $\tau$ . *DeLS-Spec (Markov)* follows the Markov head used in DSpark (Cheng et al., 2026b), where the logits of each draft token are corrected only based on the immediately preceding token. In our framework, this corresponds to generating the short-context logits using only the previous token. *Domino-FT* freezes the DFlash backbone and trains only the Domino head (Huang et al., 2026), using the same training data and number of epochs as our DeLS-Spec local head.

Although Domino-FT achieves the highest average  $\tau$ , the gap between DeLS-Spec and Domino-FT is small. On average, DFlash obtains  $\tau = 6.04$ , DeLS-Spec (RNN) improves it to 6.35, while Domino-FT reaches 6.45. Thus, omitting the residual term only leads to a 0.10 drop in average acceptance length compared with Domino-FT, while DeLS-Spec still captures 75.69% of Domino-FT’s improvement over DFlash. The  $\tau$  gain ratio is computed as  $\frac{\tau_{\text{DeLS-Spec}} - \tau_{\text{DFlash}}}{\tau_{\text{Domino-FT}} - \tau_{\text{DFlash}}}$ .

The gains are also consistent across benchmarks. DeLS-Spec (RNN) recovers more than 80% of Domino-FT’s improvement on AIME25 and HumanEval, and even surpasses Domino-FT on LCB with a  $\tau$  gain ratio of 105.56%. In addition, DeLS-Spec (RNN) consistently outperforms DeLS-Spec (Markov), improving the average  $\tau$  from 6.28 to 6.35. This shows that modeling richer short-range dependencies with an RNN local head is more effective than a one-step Markov correction, while still avoiding the full residual modeling cost of Domino-FT.

### 5.6 DO LEARNABLE $\alpha$ AND $\beta$ HELP?

We further investigate whether learning the fusion weights  $\alpha$  and  $\beta$  can bring additional gains over fixed values. As shown in Table 4,  $\alpha = \beta = 0$  corresponds to the original DFlash baseline, while  $\alpha = \beta = 0.3$  is our default setting. For the learnable variant, we initialize  $\alpha$  and  $\beta$  to 0.3 and

Table 4: Comparison between fixed and learnable fusion weights on Qwen3-4B. The fixed setting  $\alpha = \beta = 0.3$  provides the best average acceptance length, while learnable weights offer limited additional benefit and can slightly underperform the tuned fixed fusion.

$\alpha$ & $\beta$	GSM8K	MATH-500	HumanEval	MBPP	LCB	MT-Bench	Avg.
$\alpha = \beta = 0$	6.51	7.81	6.56	6.14	6.82	4.13	6.33
$\alpha = \beta = 0.3$	6.80	8.21	6.92	6.47	7.20	4.30	6.65
Learnable	6.67	8.01	6.89	6.34	7.15	4.24	6.55

Table 5: Training cost comparison on a single NVIDIA L20 GPU (48G). DeLS-Spec local heads require much less training time and memory than Domino-FT, with the Markov variant being the cheapest due to dense supervision and its minimal parameterization.

Model	Method	Supervision	Training time (h)	VRAM (GB)
Qwen3-4B	Domino-FT	anchor / block	13.4	42.6
	DeLS-Spec (RNN)	anchor / block	1.1	9.0
	DeLS-Spec (Markov)	dense supervision	0.4	6.5
Qwen3-8B	Domino-FT	anchor / block	N/A	OOM
	DeLS-Spec (RNN)	anchor / block	1.1	10.1
	DeLS-Spec (Markov)	dense supervision	0.5	5.9

optimize them for 10K steps on the training data. During this process, the target model, DFlash, and the local head are all loaded but frozen, and only  $\alpha$  and  $\beta$  are updated with the cross-entropy loss.

The learnable variant consistently improves over the DFlash baseline, increasing the average acceptance length from 6.33 to 6.55. This confirms that assigning positive weights to the local correction and unigram-prior subtraction is beneficial. However, it is still worse than our simple fixed setting  $\alpha = \beta = 0.3$ , which achieves the best average  $\tau$  of 6.65 and outperforms the learnable variant on every benchmark. For example, the fixed setting improves  $\tau$  over the learnable variant by 0.20 on MATH-500, 0.13 on GSM8K and MBPP, and 0.06 on LCB.

Appendix C reports the learned values of  $\alpha$  and  $\beta$  in Table 7. They are consistently positive and increase with draft-token position, which supports the usefulness of both terms. Nevertheless, directly optimizing these weights with cross-entropy does not translate to better acceptance length on downstream benchmarks. This suggests that the fixed  $\alpha = \beta = 0.3$  setting provides a better trade-off between effectiveness, robustness, and simplicity, avoiding the need to load all components and perform extra tuning.

## 5.7 TRAINING COST COMPARISON

We compare the training cost of Domino-FT and DeLS-Spec on a single NVIDIA L20 GPU with 48GB memory. As shown in Table 5, all methods are trained with batch size 1, accumulation steps 4, and one epoch. For Domino-FT and DeLS-Spec (RNN), we sample 256 anchors from each example to construct draft blocks. In contrast, DeLS-Spec (Markov) does not rely on anchors or block construction, and is trained with dense token-level supervision directly on the corpus.

DeLS-Spec is substantially more efficient than Domino-FT. On Qwen3-4B, Domino-FT requires 13.4 hours and 42.6GB VRAM, while DeLS-Spec (RNN) only takes 1.1 hours and 9.0GB VRAM, reducing training time by over  $12\times$  and memory usage by about  $4.7\times$ . The Markov variant is even cheaper, requiring only 0.4 hours and 6.5GB VRAM. The gap becomes more pronounced on Qwen3-8B: Domino-FT runs out of memory on a 48GB L20 GPU, whereas DeLS-Spec (RNN) still fits comfortably with 10.1GB VRAM and finishes training in 1.1 hours. DeLS-Spec (Markov) further reduces the cost to 0.5 hours and 5.9GB VRAM.

These results highlight the practical advantage of DeLS-Spec. The key reason is that the DeLS-Spec local head can be trained independently of both the target model and DFlash. In contrast, Domino-FT requires the target model to produce hidden states and DFlash to provide base logits, while the Domino head only learns the residual correction logits. As a result, Domino-FT must keep multiple large components involved during training, leading to much higher memory usage and

training time. DeLS-Spec avoids this dependency by training a lightweight local head separately, making it significantly easier to apply under limited hardware resources.

## 6 CONCLUSION

We presented **DeLS-Spec**, a decoupled long-short context method for block-parallel speculative decoding. DeLS-Spec keeps DFlash fixed as a long-context expert and adds a lightweight local head as a short-context expert. By combining their logits at inference time, it introduces intra-block causal information without retraining the draft model from scratch. The local head can be independently trained with a standard next-token prediction objective, making training cheap and modular. Since it is not one-to-one tied to a specific DFlash checkpoint, it can also be flexibly attached to compatible DFlash-style drafters. Experiments on Qwen3 models show that DeLS-Spec consistently improves speedup and average acceptance length over DFlash, demonstrating an efficient way to enhance existing block-parallel speculative decoding systems.

## 7 LIMITATIONS AND FUTURE WORK

While DeLS-Spec demonstrates significant efficiency and performance gains, our approach has several limitations that present opportunities for future research:

**Omission of Residual Interactions.** To achieve extreme training efficiency and modularity, DeLS-Spec deliberately omits the residual interaction term between the long context and the local short context. As a result, while it recovers the majority of performance improvements, its average acceptance length is slightly bounded and falls marginally short of end-to-end jointly trained methods like Domino, which explicitly learn this full residual interaction.

**Generalization to Other Parallel Drafters.** Our current empirical evaluation is primarily built upon the DFlash architecture. However, the theoretical framework of DeLS-Spec is fundamentally agnostic to the underlying draft model. Since the local head operates independently, future work will explore applying and validating DeLS-Spec on a broader range of non-autoregressive and parallel draft models beyond DFlash.

**Adaptive Logit Fusion Strategies.** Currently, DeLS-Spec employs a straightforward logit fusion mechanism with fixed hyperparameters ( $\alpha$  and  $\beta$ ). We believe the fusion process can be further optimized. Future research could explore dynamic fusion strategies, such as adaptively adjusting the local head and unigram-prior weights based on the token-level entropy or confidence scores of the long-context logits, allowing for a more context-aware balance between global semantics and local causality.

**Mitigating Exposure Mismatch in Local Heads.** As observed in our analysis, directly learning the fusion weights ( $\alpha$  and  $\beta$ ) via cross-entropy yields suboptimal inference performance compared to using fixed values. We attribute this to an exposure mismatch (or teacher-forcing bias) during training, where the local head is conditioned on ground-truth prefixes rather than its own drafted tokens. Future work could investigate techniques such as scheduled sampling or alignment-based tuning to bridge this train-test gap, potentially unlocking the full capability of learnable fusion parameters.

## REFERENCES

- Josh Achiam, Steven Adler, Sandhini Agarwal, Lama Ahmad, Ilge Akkaya, Florencia Leoni Aleman, Diogo Almeida, Janko Altenschmidt, Sam Altman, Shyamal Anadkat, et al. Gpt-4 technical report. *arXiv preprint arXiv:2303.08774*, 2023.
- Zihao An, Huajun Bai, Ziqiong Liu, Dong Li, and Emad Barsoum. Pard: Accelerating llm inference with low-cost parallel draft model adaptation. *arXiv preprint arXiv:2504.18583*, 2025.
- Zachary Ankner, Rishab Parthasarathy, Aniruddha Nrusimha, Christopher Rinard, Jonathan Ragan-Kelley, and William Brandon. Hydra: Sequentially-dependent draft heads for medusa decoding. *arXiv preprint arXiv:2402.05109*, 2024.
- Marianne Arriola, Aaron Gokaslan, Justin Chiu, Zhihan Yang, Zhixuan Qi, Jiaqi Han, Subham Sahoo, and Volodymyr Kuleshov. Block diffusion: Interpolating between autoregressive and diffusion language models. In *International Conference on Learning Representations*, volume 2025, pp. 50726–50753, 2025.
- Jacob Austin, Augustus Odena, Maxwell Nye, Maarten Bosma, Henryk Michalewski, David Dohan, Ellen Jiang, Carrie Cai, Michael Terry, Quoc Le, et al. Program synthesis with large language models. *arXiv preprint arXiv:2108.07732*, 2021.
- Samy Bengio, Oriol Vinyals, Navdeep Jaitly, and Noam Shazeer. Scheduled sampling for sequence prediction with recurrent neural networks. *Advances in neural information processing systems*, 28, 2015.
- Tianle Cai, Yuhong Li, Zhengyang Geng, Hongwu Peng, Jason D Lee, Deming Chen, and Tri Dao. Medusa: Simple llm inference acceleration framework with multiple decoding heads. *arXiv preprint arXiv:2401.10774*, 2024.
- Charlie Chen, Sebastian Borgeaud, Geoffrey Irving, Jean-Baptiste Lespiau, Laurent Sifre, and John Jumper. Accelerating large language model decoding with speculative sampling. *arXiv preprint arXiv:2302.01318*, 2023.
- Jian Chen, Yesheng Liang, and Zhijian Liu. Dflash: Block diffusion for flash speculative decoding. *arXiv preprint arXiv:2602.06036*, 2026.
- Mark Chen, Jerry Tworek, Heewoo Jun, Qiming Yuan, Henrique Ponde De Oliveira Pinto, Jared Kaplan, Harri Edwards, Yuri Burda, Nicholas Joseph, Greg Brockman, et al. Evaluating large language models trained on code. *arXiv preprint arXiv:2107.03374*, 2021.
- Shuang Cheng, Yihan Bian, Dawei Liu, Yuhua Jiang, Yihao Liu, Linfeng Zhang, Qian Yao, Zhongbo Tian, Wenhai Wang, Qipeng Guo, et al. Sdar: A synergistic diffusion-autoregression paradigm for scalable sequence generation. In *Findings of the Association for Computational Linguistics: ACL 2026*, pp. 22058–22075, 2026a.
- Xin Cheng, Xingkai Yu, Chenze Shao, Jiashi Li, Yunfan Xiong, Yi Qian, Jiaqi Zhu, Shirong Ma, Xiaokang Zhang, Jiasheng Ye, Qinyu Chen, Chengqi Deng, Jiping Yu, Damai Dai, Zhengyan Zhang, Yixuan Wei, Yixuan Tan, Wenkai Yang, Runxin Xu, Yu Wu, Zhean Xu, Xuanyu Wang, Muiyang Chen, Rui Tian, Xiao Bi, Zhewen Hao, Shaoyuan Chen, Huanqi Cao, Wentao Zhang, Anyi Xu, Huishuai Zhang, Dongyan Zhao, and Wenfeng Liang. Dspark: Confidence-scheduled speculative decoding with semi-autoregressive generation, 2026b. URL <https://arxiv.org/abs/2607.05147>.
- Yunfei Cheng, Aonan Zhang, Xuanyu Zhang, Chong Wang, and Yi Wang. Recurrent drafter for fast speculative decoding in large language models. *arXiv preprint arXiv:2403.09919*, 2024.
- Jacob K Christopher, Brian R Bartoldson, Tal Ben-Nun, Michael Cardei, Bhavya Kailkhura, and Ferdinando Fioretto. Speculative diffusion decoding: Accelerating language generation through diffusion. In *Proceedings of the 2025 Conference of the Nations of the Americas Chapter of the Association for Computational Linguistics: Human Language Technologies (Volume 1: Long Papers)*, pp. 12042–12059, 2025.

- Karl Cobbe, Vineet Kosaraju, Mohammad Bavarian, Mark Chen, Heewoo Jun, Lukasz Kaiser, Matthias Plappert, Jerry Tworek, Jacob Hilton, Reichihiro Nakano, et al. Training verifiers to solve math word problems. *arXiv preprint arXiv:2110.14168*, 2021.
- Jiatao Gu, James Bradbury, Caiming Xiong, Victor OK Li, and Richard Socher. Non-autoregressive neural machine translation. *arXiv preprint arXiv:1711.02281*, 2017.
- Dan Hendrycks, Collin Burns, Saurav Kadavath, Akul Arora, Steven Basart, Eric Tang, Dawn Song, and Jacob Steinhardt. Measuring mathematical problem solving with the math dataset. *arXiv preprint arXiv:2103.03874*, 2021.
- Geoffrey E Hinton. Training products of experts by minimizing contrastive divergence. *Neural computation*, 14(8):1771–1800, 2002.
- Lanxiang Hu, Zhaoxiang Feng, Yulun Wu, Haoran Yuan, Yujie Zhao, Yu-Yang Qian, Bojun Wang, Peng Zhao, Daxin Jiang, Yibo Zhu, Tajana Rosing, and Hao Zhang. Jetspec: Breaking the scaling ceiling of speculative decoding with parallel tree drafting, 2026. URL <https://arxiv.org/abs/2606.18394>.
- Jianuo Huang, Yaojie Zhang, Qituan Zhang, Hao Lin, Hanlin Xu, and Linfeng Zhang. Domino: Decoupling causal modeling from autoregressive drafting in speculative decoding. *arXiv preprint arXiv:2605.29707*, 2026.
- Naman Jain, King Han, Alex Gu, Wen-Ding Li, Fanjia Yan, Tianjun Zhang, Sida Wang, Armando Solar-Lezama, Koushik Sen, and Ion Stoica. Livecodebench: Holistic and contamination free evaluation of large language models for code. In *The Thirteenth International Conference on Learning Representations*, 2025. URL <https://openreview.net/forum?id=chfJJYC3iL>.
- Yaniv Leviathan, Matan Kalman, and Yossi Matias. Fast inference from transformers via speculative decoding. In *International Conference on Machine Learning*, pp. 19274–19286. PMLR, 2023.
- Guanghao Li, Zhihui Fu, Min Fang, Qibin Zhao, Ming Tang, Chun Yuan, and Jun Wang. Diffuspec: Unlocking diffusion language models for speculative decoding. In *Findings of the Association for Computational Linguistics: ACL 2026*, pp. 20896–20910, 2026a.
- Yuhui Li, Fangyun Wei, Chao Zhang, and Hongyang Zhang. Eagle: Speculative sampling requires rethinking feature uncertainty. *arXiv preprint arXiv:2401.15077*, 2024a.
- Yuhui Li, Fangyun Wei, Chao Zhang, and Hongyang Zhang. Eagle-2: Faster inference of language models with dynamic draft trees. In *Proceedings of the 2024 conference on empirical methods in natural language processing*, pp. 7421–7432, 2024b.
- Yuhui Li, Fangyun Wei, Chao Zhang, and Hongyang Zhang. Eagle-3: Scaling up inference acceleration of large language models via training-time test. *Advances in Neural Information Processing Systems*, 38:136737–136756, 2026b.
- Aixin Liu, Bei Feng, Bing Xue, Bingxuan Wang, Bochao Wu, Chengda Lu, Chenggang Zhao, Chengqi Deng, Chenyu Zhang, Chong Ruan, et al. Deepseek-v3 technical report. *arXiv preprint arXiv:2412.19437*, 2024.
- Fuliang Liu, Xue Li, Ketai Zhao, Yinxi Gao, Ziyang Zhou, Zhonghui Zhang, Zhibin Wang, Wanchun Dou, Sheng Zhong, and Chen Tian. Dart: Diffusion-inspired speculative decoding for fast llm inference. *arXiv preprint arXiv:2601.19278*, 2026.
- Jingyu Liu, Xin Dong, Zhifan Ye, Rishabh Mehta, Yonggan Fu, Vartika Singh, Jan Kautz, Ce Zhang, and Pavlo Molchanov. Tidar: Think in diffusion, talk in autoregression. *arXiv preprint arXiv:2511.08923*, 2025.
- Xupeng Miao, Gabriele Oliaro, Zhihao Zhang, Xinhao Cheng, Zeyu Wang, Zhengxin Zhang, Rae Ying Yee Wong, Alan Zhu, Lijie Yang, Xiaoxiang Shi, et al. Specinfer: Accelerating large language model serving with tree-based speculative inference and verification. In *Proceedings of the 29th ACM International Conference on Architectural Support for Programming Languages and Operating Systems, Volume 3*, pp. 932–949, 2024.

- Shen Nie, Fengqi Zhu, Zebin You, Xiaolu Zhang, Jingyang Ou, Jun Hu, Jun Zhou, Yankai Lin, Ji-Rong Wen, and Chongxuan Li. Large language diffusion models. *Advances in Neural Information Processing Systems*, 38:50608–50646, 2026.
- Peer Rheinboldt, Frédéric Berdoz, and Roger Wattenhofer. Treeflash: Parallel ar-approximation for faster speculative decoding. *arXiv preprint arXiv:2606.03819*, 2026.
- Liran Ringel and Yaniv Romano. Accelerating speculative decoding with block diffusion draft trees. *arXiv preprint arXiv:2604.12989*, 2026.
- Jameson Sandler, Jacob K Christopher, Thomas Hartvigsen, and Ferdinando Fioretto. Specdiff-2: Scaling diffusion drafter alignment for faster speculative decoding. *arXiv preprint arXiv:2511.00606*, 2025.
- Mitchell Stern, Noam Shazeer, and Jakob Uszkoreit. Blockwise parallel decoding for deep autoregressive models. *Advances in Neural Information Processing Systems*, 31, 2018.
- Zhiqing Sun, Zhuohan Li, Haoqing Wang, Di He, Zi Lin, and Zhihong Deng. Fast structured decoding for sequence models. *Advances in Neural Information Processing Systems*, 32, 2019.
- Rohan Taori, Ishaan Gulrajani, Tianyi Zhang, Yann Dubois, Xuechen Li, Carlos Guestrin, Percy Liang, and Tatsunori B Hashimoto. Alpaca: A strong, replicable instruction-following model. *Stanford Center for Research on Foundation Models*. <https://crfm.stanford.edu/2023/03/13/alpaca.html>, 3(6):7, 2023.
- Philippe Tillet, Hsiang-Tsung Kung, and David Cox. Triton: an intermediate language and compiler for tiled neural network computations. In *Proceedings of the 3rd ACM SIGPLAN International Workshop on Machine Learning and Programming Languages*, pp. 10–19, 2019.
- Zhuofan Wen, Shangdong Gui, and Yang Feng. Speculative decoding with ctc-based draft model for llm inference acceleration. *Advances in Neural Information Processing Systems*, 37:92082–92100, 2024.
- Thomas Wolf, Lysandre Debut, Victor Sanh, Julien Chaumond, Clement Delangue, Anthony Moi, Pierric Cistac, Tim Rault, Rémi Louf, Morgan Funtowicz, et al. Huggingface’s transformers: State-of-the-art natural language processing. *arXiv preprint arXiv:1910.03771*, 2019.
- Tianyu Wu, Yu Yao, Zhenting Qi, Han Zheng, Zhuohan Wang, Haoran Ma, Lawrence Liao, Himabindu Lakkaraju, Ju Li, and Yilun Du. D-pace: Dynamic position-aware cross-entropy for parallel speculative drafting. *arXiv preprint arXiv:2605.18810*, 2026.
- An Yang, Anfeng Li, Baosong Yang, Beichen Zhang, Binyuan Hui, Bo Zheng, Bowen Yu, Chang Gao, Chengen Huang, Chenxu Lv, et al. Qwen3 technical report. *arXiv preprint arXiv:2505.09388*, 2025.
- Yifan Zhang and Team Math-AI. American invitational mathematics examination (aime) 2025, 2025.
- Lianmin Zheng, Wei-Lin Chiang, Ying Sheng, Siyuan Zhuang, Zhanghao Wu, Yonghao Zhuang, Zi Lin, Zhuohan Li, Dacheng Li, Eric Xing, et al. Judging llm-as-a-judge with mt-bench and chatbot arena. *Advances in neural information processing systems*, 36:46595–46623, 2023.
- Yongchao Zhou, Kaifeng Lyu, Ankit Singh Rawat, Aditya Krishna Menon, Afshin Rostamizadeh, Sanjiv Kumar, Jean-François Kagy, and Rishabh Agarwal. Distillspec: Improving speculative decoding via knowledge distillation. In *International Conference on Learning Representations*, volume 2024, pp. 32011–32050, 2024.

## A IMPLEMENTATION DETAILS

**Local Head Implementation.** We instantiate  $p_S(x_i | z_i)$  with a lightweight local head over the local draft prefix. Since the local head is evaluated autoregressively during inference, we use a low-rank bottleneck to reduce the sequential computation cost, following the design choice in Domino and DSpark (Huang et al., 2026; Cheng et al., 2026b). For the RNN variant, token ids are mapped by the frozen target embedding table and passed through a one-layer bias-free GRU; the final hidden state is projected to a low-rank state with SiLU activation and then mapped to vocabulary logits:

$$r_i = \text{SiLU}(W_{\text{rank}} \text{GRU}(E_{\text{tgt}}(z_i))), \quad \ell_S^{\text{RNN}}(x_i | z_i) = W_{\text{vocab}} r_i.$$

For the Markov variant, we directly look up a low-rank state from the most recent token and multiply it with a low-rank vocabulary head:

$$r_i = E_M(x_{i-1}), \quad \ell_S^{\text{Markov}}(x_i | z_i) = r_i W_M^T,$$

where  $E_M, W_M \in \mathbb{R}^{|\mathcal{V}| \times d_r}$ . Both variants output full-vocabulary logits and are trained with the same next-token prediction objective as the short-context model. The hyperparameters for the local head are summarized in Table 6.

**Unigram Prior Estimation.** We construct a fixed unigram log-prior over target tokens using the same tokenizer and chat-template preprocessing as training. For each training sequence, we count only tokens whose loss mask equals one, i.e., assistant-response tokens that contribute to the supervised objective. Let  $c(v)$  denote the resulting count for vocabulary item  $v$ . We form a smoothed prior

$$\tilde{p}_0(v) = \frac{c(v) + \lambda}{\sum_{v'} (c(v') + \lambda)},$$

where we use additive smoothing with  $\lambda = 1.0$  by default. We then use  $b_0(v) = \log \tilde{p}_0(v)$  as a fixed vocabulary-level bias.

Table 6: Training hyperparameters for the local head.

Hyperparameter	Value
block-size	16
num-anchors	512
local-gru-hidden-dim	1024
local-rank	256
local-rank-activation	SiLU
loss-decay-gamma	7.0
max-length	3072
batch-size	4
accumulation-steps	1
learning-rate	6e-4
num-epochs	1

## B PROOF OF THE PRODUCT-OF-EXPERTS FACTORIZATION

In Section 4.1, we introduce the exact factorization of the conditional probability  $p(x_i | y, z_i)$ . Here, we provide the step-by-step derivation for this decomposition.

Starting from Bayes' theorem, the conditional probability of the candidate token  $x_i$  given the long context  $y$  and the short context  $z_i$  can be written as:

$$p(x_i | y, z_i) = \frac{p(y, z_i | x_i) p(x_i)}{p(y, z_i)}. \quad (11)$$

We can multiply both the numerator and the denominator by the product of the marginals  $p(y) p(z_i)$  and the conditional probabilities  $p(y | x_i) p(z_i | x_i)$ :

$$p(x_i | y, z_i) = \frac{p(y, z_i | x_i) p(x_i)}{p(y, z_i)} \cdot \frac{p(y | x_i) p(z_i | x_i)}{p(y | x_i) p(z_i | x_i)} \cdot \frac{p(y) p(z_i)}{p(y) p(z_i)}. \quad (12)$$

By rearranging the terms, we group them into three distinct factors:

$$p(x_i | y, z_i) = \left[ \frac{p(y | x_i) p(z_i | x_i) p(x_i)}{p(y) p(z_i)} \right] \cdot \frac{p(y) p(z_i)}{p(y, z_i)} \cdot \frac{p(y, z_i | x_i)}{p(y | x_i) p(z_i | x_i)}. \quad (13)$$

Recall that by applying Bayes' theorem to the individual contexts, we can express the conditional probabilities of  $x_i$  as:

$$p(x_i | y) = \frac{p(y | x_i) p(x_i)}{p(y)} \quad \text{and} \quad p(x_i | z_i) = \frac{p(z_i | x_i) p(x_i)}{p(z_i)}. \quad (14)$$

Multiplying these two equations together and dividing by the unigram prior  $p(x_i)$  yields the exact expression inside the square brackets of Equation 13:

$$\frac{p(x_i | y) p(x_i | z_i)}{p(x_i)} = \frac{p(y | x_i) p(z_i | x_i) p(x_i)}{p(y) p(z_i)}. \quad (15)$$

Substituting this equivalence back into Equation 13 gives the final exact equality:

$$p(x_i | y, z_i) = \frac{p(x_i | y) p(x_i | z_i)}{p(x_i)} \cdot \frac{p(y) p(z_i)}{p(y, z_i)} \cdot \frac{p(y, z_i | x_i)}{p(y | x_i) p(z_i | x_i)}. \quad (16)$$

This completes the proof.

## C ANALYSIS OF LEARNABLE $\alpha$ AND $\beta$

Table 7 reports the learned values of  $\alpha$  and  $\beta$  at different draft-token positions. We observe that both weights become relatively large at later positions. For example,  $\alpha$  increases from 0.547 at position 2 to around 0.762 after position 12, while  $\beta$  also increases from 0.512 to around 0.613. This trend suggests that the learned fusion weights assign increasingly higher importance to the local head and the unigram-prior correction for later draft tokens.

A possible explanation is the mismatch introduced by teacher forcing during training (Bengio et al., 2015). When optimizing  $\alpha$  and  $\beta$  on the training data, later positions are conditioned on longer ground-truth prefixes. Under this setting, the local head can exploit more accurate short-context information and may appear more reliable than DFlash for predicting later draft tokens. As a result, the optimization tends to assign larger  $\alpha$  and  $\beta$  values to later positions.

However, this advantage may not fully transfer to inference. During speculative decoding, later draft tokens are conditioned on previously drafted tokens rather than ground-truth tokens, which introduces exposure bias. Therefore, overly large learned weights at later positions may overestimate the reliability of the local correction and lead to suboptimal acceptance length. This explains why the learnable variant in Table 4 improves over the DFlash baseline but still underperforms the fixed setting  $\alpha = \beta = 0.3$ . The fixed setting is less sensitive to the teacher-forcing bias and provides a more robust choice for inference.

Table 7: Learnable  $\alpha$  and  $\beta$  values by position.

Position	$\alpha$	$\beta$
2	0.547	0.512
3	0.594	0.523
4	0.633	0.539
5	0.672	0.559
6	0.699	0.578
7	0.715	0.586
8	0.730	0.598
9	0.742	0.605
10	0.750	0.613
11	0.754	0.613
12	0.762	0.613
13	0.762	0.617
14	0.762	0.613
15	0.762	0.613

## D COMPARISON OF ACCEPTANCE RATE RESULTS

Table 8 provides a position-wise view of the acceptance behavior on Qwen3-4B at temperature 0. Unlike the average acceptance length  $\tau$  reported in Table 1, the quantity  $rate_i = P(\text{acceptance length} \geq i)$  measures the probability that verification accepts at least the first  $i$  draft tokens. It therefore describes the tail of the accepted draft length distribution: improvements at larger positions indicate that the method more often preserves longer consecutive draft spans, which is the direct source of higher average acceptance length and decoding speedup.

The results show that DeLS-Spec improves the acceptance curve over DFlash across almost all nontrivial positions. The first position is accepted by both methods by definition, and the second position is nearly unchanged (81.45% versus 81.63%). From position 3 onward, however, DeLS-Spec consistently achieves higher acceptance rates. The gains are largest in the middle of the draft block, reaching about 2.6 percentage points around positions 5–6, and remain positive even at the end of the block, with a 1.40 percentage-point improvement at position 16. This pattern supports the main hypothesis of DeLS-Spec: the local head and unigram-prior correction do not merely improve isolated early predictions, but make the draft sequence locally more coherent so that verification can accept longer prefixes.

Table 8: Acceptance-rate comparison by position on Qwen3-4B at temperature 0, where  $rate_i = P(\text{acceptance length} \geq i)$ .

Position	DFlash	DeLS-Spec	DeLS-Spec - DFlash
1	100.00%	100.00%	+0.00%
2	81.63%	81.45%	-0.18%
3	63.98%	65.10%	+1.13%
4	50.65%	52.69%	+2.03%
5	41.26%	43.80%	+2.54%
6	34.38%	36.99%	+2.61%
7	29.26%	31.63%	+2.37%
8	25.15%	27.49%	+2.34%
9	22.02%	24.11%	+2.10%
10	19.45%	21.24%	+1.79%
11	17.14%	18.85%	+1.71%
12	15.26%	16.83%	+1.57%
13	13.44%	14.95%	+1.51%
14	11.96%	13.42%	+1.46%
15	10.51%	11.96%	+1.45%
16	9.22%	10.62%	+1.40%